ERRα promotes breast cancer cell dissemination to bone by increasing RANK expression in primary breast tumors

G Vargas, M Bouchet, L Bouazza, P Reboul, C Boyault, M Gervais, C Kan, C Benetollo, M Brevet, M Croset, et al.

Oncogene
https://doi.org/10.1038/s41388-018-0579-3

ARTICLE

ERRα promotes breast cancer cell dissemination to bone by increasing RANK expression in primary breast tumors

G. Vargas[1,2] · M. Bouchet[1,2,3] · L. Bouazza[1,2] · P. Reboul[4] · C. Boyault[5] · M. Gervais[1,2] · C. Kan[1,2,6] · C. Benetollo[2,7] · M. Brevet[1,8] · M. Croset[1,2] · M. Mazel[9] · L. Cayrefourcq[9] · S. Geraci[1,2] · S. Vacher[10] · F. Pantano[11] · M. Filipits[12] · K. Driouch[10] · I. Bieche[10] · M. Gnant[12] · W. Jacot[13] · J. E. Aubin[14] · M. Duterque-Coquillaud[15] · C. Alix-Panabières[9] · P. Clézardin[1,2] · E. Bonnelye[1,2]

Received: 18 January 2018 / Accepted: 20 October 2018

Abstract

Bone is the most common metastatic site for breast cancer. Estrogen-related-receptor alpha (ERRα) has been implicated in cancer cell invasiveness. Here, we established that ERRα promotes spontaneous metastatic dissemination of breast cancer cells from primary mammary tumors to the skeleton. We carried out cohort studies, pharmacological inhibition, gain-of-function analyses in vivo and cellular and molecular studies in vitro to identify new biomarkers in breast cancer metastases. Meta-analysis of human primary breast tumors revealed that high ERRα expression levels were associated with bone but not lung metastases. ERRα expression was also detected in circulating tumor cells from metastatic breast cancer patients. ERRα overexpression in murine 4T1 breast cancer cells promoted spontaneous bone micro-metastases formation when tumor cells were inoculated orthotopically, whereas lung metastases occurred irrespective of ERRα expression level. In vivo, Rank was identified as a target for ERRα. That was confirmed in vitro in Rankl stimulated tumor cell invasion, in mTOR/pS6K phosphorylation, by transactivation assay, ChIP and bioinformatics analyses. Moreover, pharmacological inhibition of ERRα reduced primary tumor growth, bone micro-metastases formation and Rank expression in vitro and in vivo. Transcriptomic studies and meta-analysis confirmed a positive association between metastases and ERRα/RANK in breast cancer patients and also revealed a positive correlation between ERRα and $BRCA1^{mut}$ carriers. Taken together, our results reveal a novel ERRα/RANK axis by which ERRα in primary breast cancer promotes early dissemination of cancer cells to bone. These findings suggest that ERRα may be a useful therapeutic target to prevent bone metastases.

Introduction

Metastases are the primary cause of death [1] and in breast cancer (BCa), bone is the most common metastatic site [2]. Bone metastases (BM) detection often occurs in the

Electronic supplementary material The online version of this article (https://doi.org/10.1038/s41388-018-0579-3) contains supplementary material, which is available to authorized users.

✉ E. Bonnelye
edith.bonnelye@inserm.fr

1 INSERM-UMR1033, Lyon, France
2 University of Lyon1, Lyon, France
3 IGFL, Lyon, France
4 UMR7365-CNRS-Université de Lorraine, Nancy, France
5 Institute for Advanced Biosciences, Grenoble, France
6 Center for Cancer Research, University of Sydney, Sydney, Australia
7 INSERM-U1028-CNRS-UMR5292, Lyon, France
8 Centre de Biologie et de Pathologie Est, Bron, France
9 EA2415-Institut Universitaire de Recherche Clinique, Montpellier, France
10 Department of Genetics, Institut-Curie, Paris, France
11 University-Campus-Bio-Medico, Rome 00128, Italy
12 Department of Surgery and Comprehensive Cancer Center, Medical-University of Vienna, Vienna, Austria
13 Montpellier Cancer Institute, Montpellier, France
14 University of Toronto, Toronto, Canada
15 UMR8161/CNRS-Institut de Biologie de Lille, Lille, France

Published online: 26 November 2018

symptomatic stage and when they are diagnosed, the prognosis for the patient is generally poor and associated with significant morbidity. Unfortunately, current treatments for BM that rely on anti-resorptive agents are only palliative underlining the need for early detection for early intervention [3–5].

Nuclear steroid receptors are transcription factors that comprise both ligand-dependent molecules, such as estrogen receptors (ERs) and a large number of so-called orphan receptors, for which no natural ligands have yet been identified [6]. The estrogen-related receptor alpha (ERRα) shares structural similarities with ERα/β, but it does not bind estrogens [6]. Indeed, sequence alignment of ERRα and the ERs reveals a high similarity (68%) in the 66 amino acids of the DNA-binding domain, but only a moderate similarity (36%) in the ligand-binding domain [7]. Although ERRα activity is decreased by synthetic molecules, such as the inverse-agonists XCT790 or C29, no natural ligand has yet been found [8, 9].

ERRα is known to regulate the adaptive bioenergetics response [10]. It is widely expressed in both healthy tissues and a range of cancerous cells [11–14]. Notably, ERRα-positive tumors were associated with more invasive disease and higher risk of recurrences [11–13]. In addition to angiogenesis, ERRα is mainly linked to tumor cell invasion [13–15]. ERRα is also highly expressed in skeletal tissues where it regulates osteoblast/osteoclast physiology [16–19]. In BM, we have reported that overexpression of ERRα in triple-negative BCa cells and castration-resistant prostate cancer cells results in either the inhibition or the activation of tumor cell progression in bone, respectively [20, 21]. Here, we assess whether ERRα in primary breast tumors regulates the molecular mechanisms that drive BCa cell homing to bone.

Results

High ERRα protein expression levels in primary tumors are associated with bone relapse in BCa patients

We assessed ERRα protein expression levels in primary tumors from patients of the ABCSG trial 6 cohort, a prospective, randomized clinical study of postmenopausal patients with hormone receptor-positive early-stage BCa, treated with tamoxifen-aminoglutethimide and followed for up to 15 years [22]. Kaplan–Meier analysis showed that high levels of ERRα protein expression (Fig. 1A, B) correlated with lower distant recurrence-free survival (%) ($n = 100$). After establishing conditions for ERRα detection using cell lines (Supplementary Fig. S1), we also detected ERRα expression in circulating tumor cells (CTCs) (Fig. 1C), supporting the hypothesis that ERRα present in CTCs may be involved in the metastatic process. We then analyzed the ERRα transcriptional profile in the NKI-295 cohort that includes primary BCa patients with known location of the first distant metastasis site [23] (Supplementary Table S1). Univariate Cox proportional hazard model analysis indicated that ERRα expression is associated with metastases-free survival (MFS) and bone metastases free-survival (BMFS) but not with lung metastases free-survival (LMFS) (Table 1). Kaplan–Meier curves also demonstrated that high *ERR*α expression is correlated with a decrease in BMFS but not LMFS (Fig. 1D, E). Neither ERRβ nor ERRγ mRNA expression levels correlated with MFS, BMFS, or LMFS (Table 1).

ERRα in BCa cells promotes spontaneous bone micro-metastases formation in vivo

To assess the role of *ERR*α in the early steps of metastatic dissemination of BCa, we used the murine 4T1 BCa cell line, from which cells spontaneously metastasize from primary tumor to lung and bone [24, 25]. Three independent 4T1 clones overexpressing-ERRα (4T1-ERRα) and two empty vector controls (4T1-CT) were isolated (Fig. 2Aa). In parallel, three 4T1-ERRαAF2 clones in which ERRα acts dominant-negatively, were obtained (Fig. 2Ab) [20, 21]. Analysis of primary breast tumors (Fat-Pad(FP)) indicated greater tumor progression in mice with 4T1-ERRα-FP compared to 4T1-CT-FP (Fig. 2Ba–b, C, D), and 4T1-ERRαAF2-FP tumors (Fig. 2Ba, c, E, F). In agreement with previous data [26], we found *Vegf-a* expression increased in 4T1-ERRα-FP tumors (Supplementary Fig. S2), as did expression of genes implicated in glycolysis and lactate metabolism (Supplementary Table S2). Culturing cells collected from crushed bones of mice kept for an additional 21 days post-primary tumor resection and counting colonies [25] revealed greater tumor cell colonization of bone (TCB) by 4T1-ERRα-FP (Fig. 2G, Supplementary Fig. S3A), with higher incidence of dissemination to bone with 4T1-ERRα cells (77% versus 12% (4T1-CT)) (Fig. 2H) and a higher number of TCB (Fig. 2I). No significant difference was observed between 4T1-ERRαAF2 cells and 4T1-CT cells (Fig. 2H, I, Supplementary Fig. S3B). In contrast, histological assessment of lung metastases (LM) revealed no difference in the number or incidence of lung colonies (Fig. 2J–L) or metastases surface amongst all groups (Supplementary Fig. S3C,D), in spite of maintenance of ERRα overexpression in 4T1-ERRα-LM versus 4T1-CT-LM (Supplementary Fig. S3E). These pre-clinical data confirm a correlation between ERRα expression level and BMFS but not LMFS (Fig. 1D, E; Table 1).

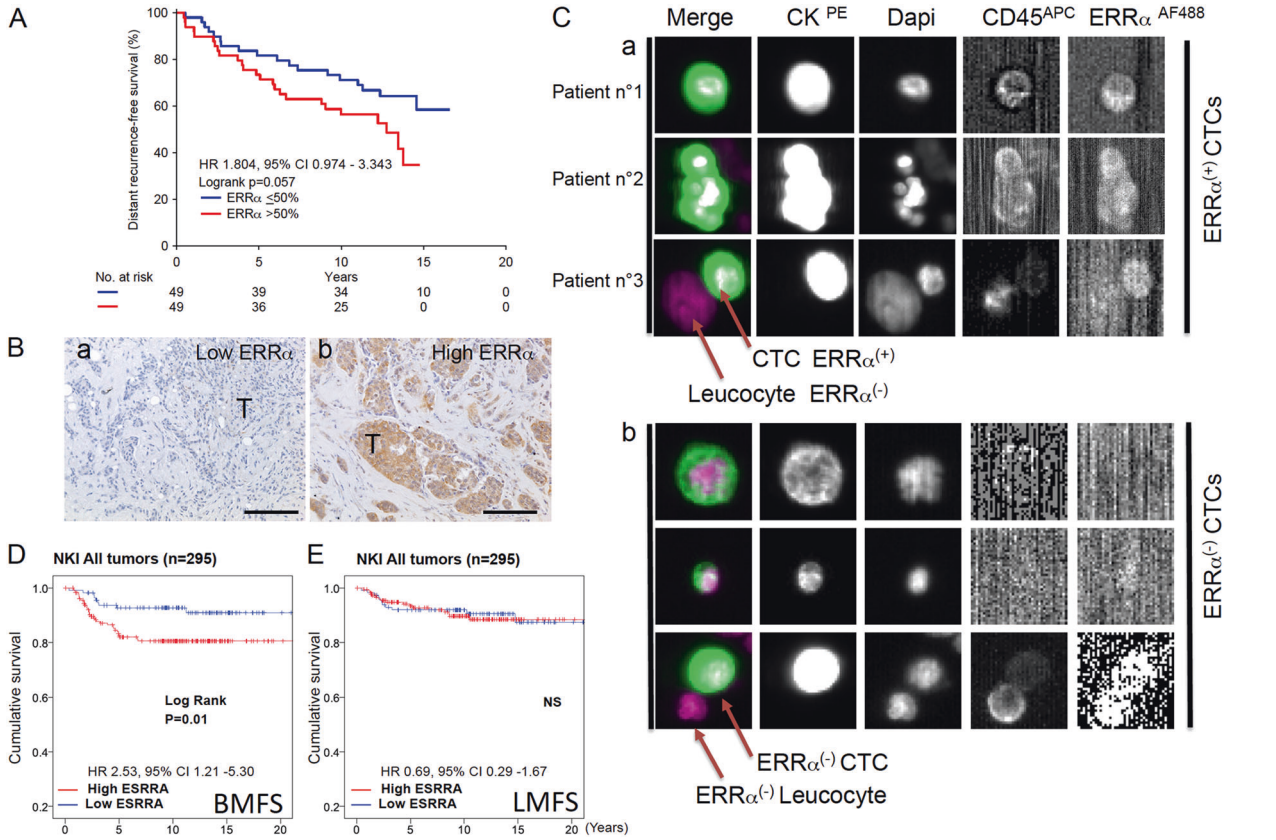

Fig. 1 ERRα is a bone metastases-associated gene in BCa. **A** Kaplan–Meier curves show correlation between high expression of ERRα, categorized with median value, and distant recurrence-free survival in patients treated with tamoxifen alone or aminoglutethimide with tamoxifen ($n = 100$). **B** Visualization of ERRα protein expression at low (**a**) and high level (**b**) by IHC on sections of primary breast tumor. **C** Representative EpCAM$^{(+)}$, pan-keratin$^{(+)}$ (K-PE), CD45$^{(-)}$ CTCs and ERRα-AF488$^{(+)/(-)}$ from metastatic BCa patients detected by the CellSearch® System. DAPI was used for nuclear counter staining. **D** Kaplan–Meier curves constructed after segmentation into two groups on the basis of the median value for ERRα expression show correlation between high expression of ERRα and lower bone metastases free-survival (BMFS) in NKI cohort ($n = 295$, $P = 0.01$); Low ≤ 50% quartile; high ≥ 50%. **E** No correlation was found between high level of ERRα and lung metastases free-survival (LMFS)

ERRα regulates Rank expression in BCa cells

To explore the mechanism underlying the ability of ERRα to promote homing of cancer cells to bone in vivo, we quantified in FP-tumors transcriptional expression levels of several markers known to be involved in the metastatic process (Fig. 3A; Supplementary Table S2). As expected, 4T1-ERRα-cells undergo epithelial–mesenchymal transition (EMT) (Supplementary Table S2) [13]. Interestingly, expression of receptor activator of nuclear factor κ B (*Rank*) mRNA was higher in 4T1-ERRα-FP [27–29], whereas no difference was observed in the mRNA expression of *Cxcr4* which had been implicated in lung tropism (Fig. 3A). Consistent with these data, Rank protein expression was also higher in 4T1-ERRα-FP (Fig. 3Ba, b). Rank protein expression was also much higher in 4T1-ERRα cells in bone metastases (BM) (Fig. 3Ca, c, Cb, d) induced by intra-arterial (IA) injection of cells, but was barely detectable in the LM elicited by either cell population (Fig. 3Da, c, Db, d; Supplementary Fig. S4A,B,C), suggesting a major role of Rank for BCa cell anchorage and colonization in bone. Culturing cells collected from crushed bones and lungs confirmed *Rank* mRNA up-regulation in 4T1-ERRα-BM but not in LM (Fig. 3E). The fact that Rank-ligand (*Rankl*) expression was significantly higher in bone versus lung (Fig. 3F) further suggests their involvement in BCa cell colonization of bone but not lung. *RANK* regulation by ERRα was confirmed in two human BCa cell lines: the MCF7 line engineered to overexpress full-length (MCF7-ERRα) or truncated (MCF7-ERRαAF2) human *ERRα* compared to the empty vector control (MCF7-CT) (Fig. 3G, H) and the MDA-MB-231-B02, known to metastasize only to bone (Fig. 3I) [20]. Moreover, C29 inhibited *Rank* mRNA expression in 4T1 and MCF7 parental cells (Fig. 3J–M) [9, 30]. *ERRα* and *RANK* mRNA were also co-expressed in the human BC-M1 disseminated tumor cell

Table 1 ERRα is a bone metastases-associated gene in BCa

Parameter	Metastasis free survival			Bone metastasis free survival			Lung metastasis free survival		
	P-value	HR	FDR	*P*-value	HR	FDR	*P*-value	HR	FDR
ESRRA	**0.008**	5.80	0.025	**0.003**	23.72	0.009	0.215	5.192	0.55
ESRRG	0.08	0.55	0.118	0.56	0.72	0.838	0.366	0.531	0.55
ESRRB	0.39	2.5	0.392	0.94	1.15	0.941	0.673	0.346	0.673

Cohort NKI ($n = 295$), Univariate Cox proportional hazards model, Wald statistic

Univariate Cox proportional hazard model analysis revealed that ERRα mRNA expression is associated with metastases free survival (MFS) and bone metastases free survival (BMFS) ($n = 295$, $P = 0.008$ and $P = 0.001$, respectively) while no link was found in lung metastases free-survival (LMFS)

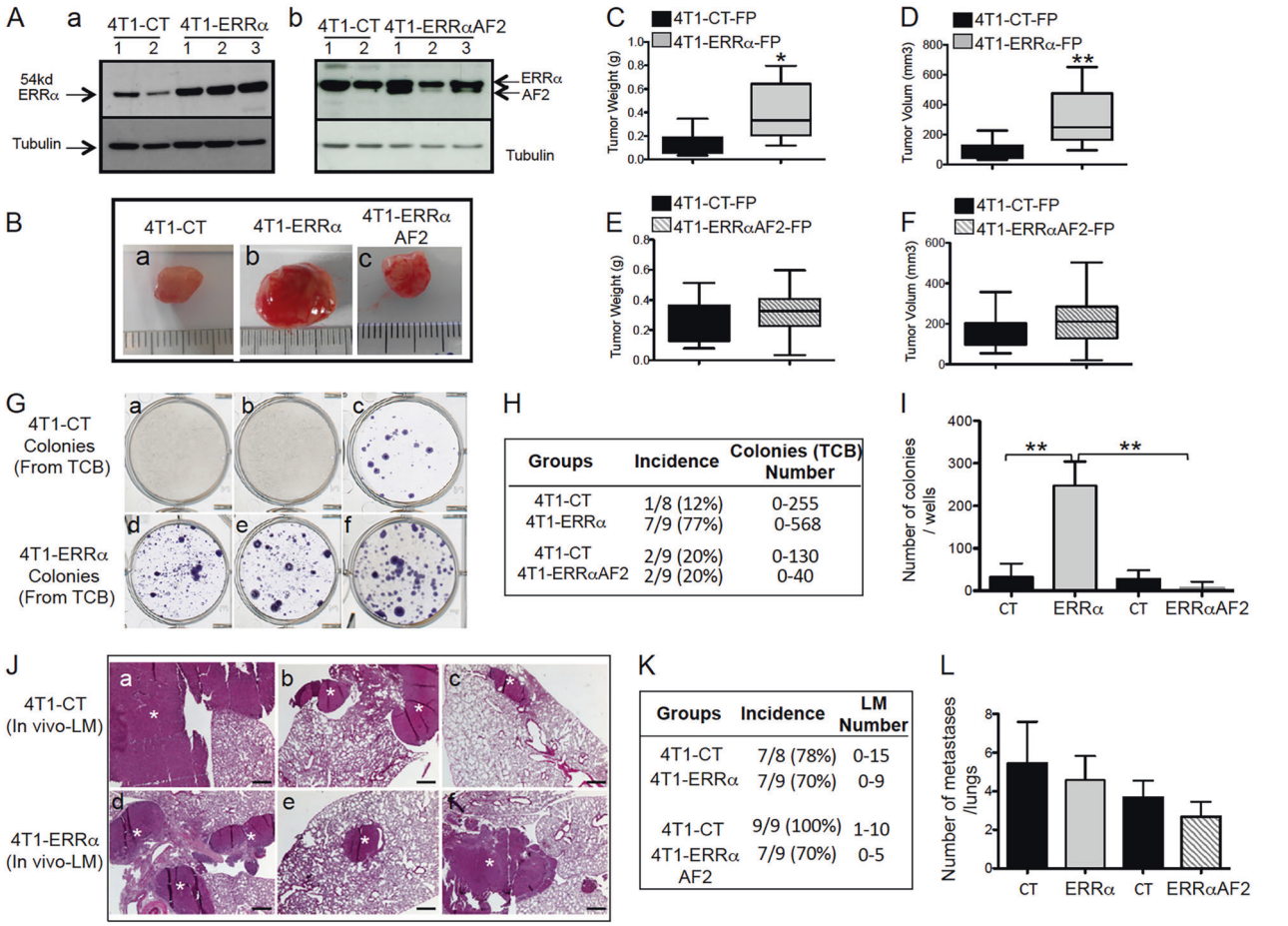

Fig. 2 ERRα promotes BCa cell homing to bone in vivo. **A** (**a**) Three independent clones (4T1-ERRα 1–3) overexpressing full-length ERRα and two control clones with empty vector (4T1-CT 1–2) were obtained after stable transfection of 4T1 cells. ERRα (~54kDa) expression was assessed by Western blotting and compared to α-tubulin as a protein loading control showing the *ERR*α protein band increased in 4T1-ERRα (1–3) compared to 4T1-CT (1, 2) cells. (**b**) Three independent 4T1-ERRαAF2 clones (ERRα dominant-negative) and two control clones (4T1-CT clones 1,2) (empty vector) were obtained and a band with slightly lower molecular weight, corresponding to the expected size for truncation of the AF2-AD domain (42aa) (co-activators binding domain), was present in 4T1-AF2 cells. **B** 4T1-ERRα (pool of three clones), 4T1-CT (pool of two clones), or 4T1-ERRαAF2 (pool of three clones) cells were inoculated into the mammary gland fat pad of BALB/c mice. Greater tumor expansion was observed in mice with 4T1-ERRα-FP. **C–F** Weight and volume of tumors dissected at end-point ($n = 10$, Mann–Whitney, weight: $P = 0.0156$; volume: $P = 0.0074$ for 4T1-ERRα), no difference was observed in mice with 4T1-ERRαAF2-FP ($n = 9$). **G** After resection, animals were kept for 21 days, bones were then crushed and released cells were cultured for 3 weeks. **H**, **I** Counting of tumor cells that colonized the bone (TCB) revealed a high incidence with 4T1-ERRα cells (**H**) that was associated with an increase in TCB number (ANOVA: $p < 0.0001$ and Mann–Whitney, $P = 0.0083$ ($n = 9$), 262 ± 175 (4T1-ERRα) versus 32 ± 55 (4T1-CT); $P = 0.006$, 4T1-ERRα versus 4T1-ERRαAF2) (**I**). Incidence and TCB number were similar in 4T1-CT and 4T1-ERRαAF2 cells. **J–L** Histological assessment of lung metastases (LM) (**J**) shows no difference between LM incidence (**K**) and LM number/lungs (**L**) ($n = 9$). Asterisk represents lung metastases

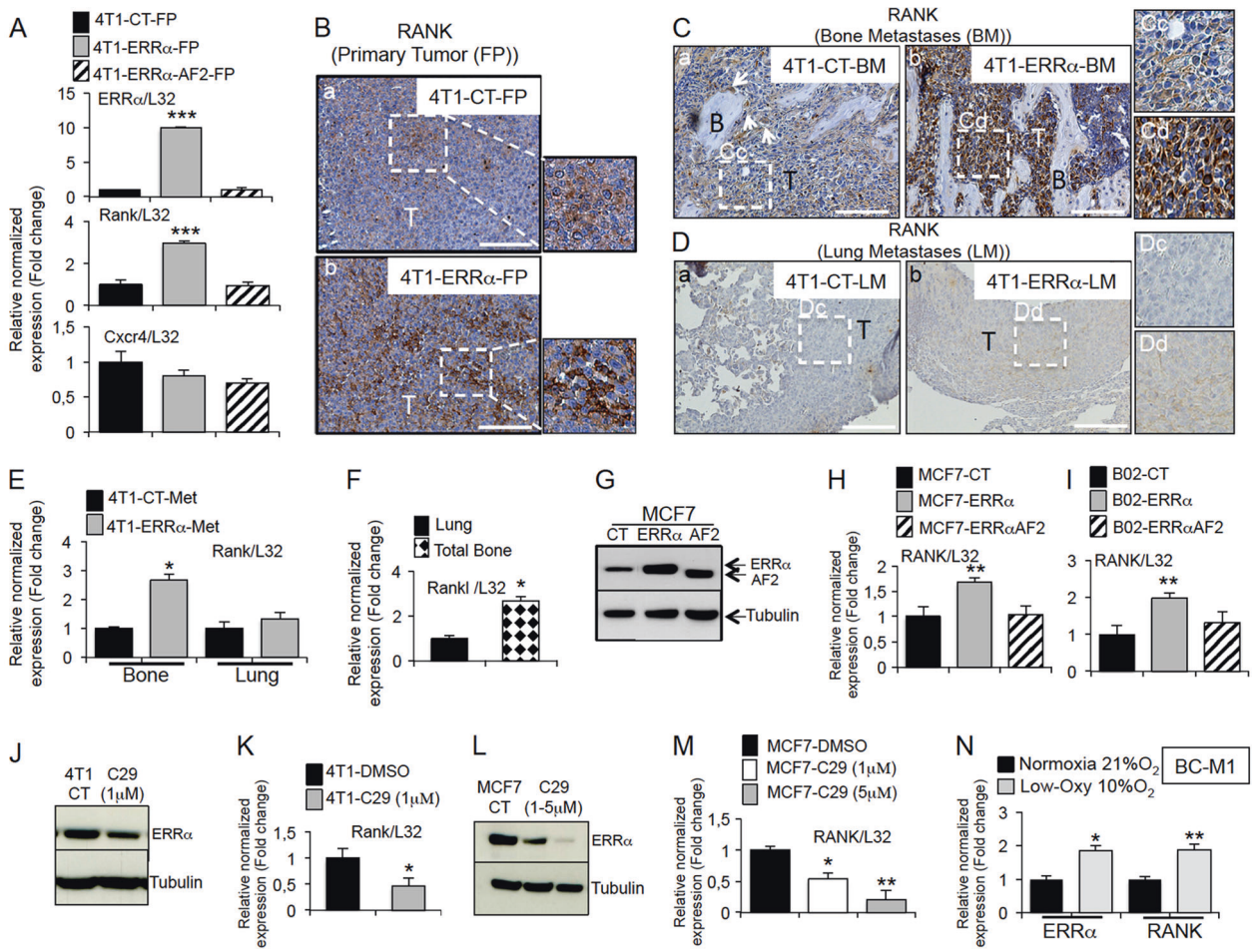

Fig. 3 Correlation between ERRα and Rank expression in BCa cells. **A** Real-time PCR performed on mRNA extracted from 4T1 primary tumors ($n = 3$ for all conditions) confirmed increased expression of ERRα in 4T1-ERRα-FP and show increased expression of *Rank* by *ERRα* (ANOVA: $P < 0.0001$ and unpaired *t*-test $P < 0.0001$ for both *ERRα* and *Rank*). *Cxcr4* mRNA expression was not altered. **B** Increased expression of Rank was visualized by IHC in 4T1-ERRα-FP (**b**) compared to 4T1-CT-FP (**a**) and in bone metastases (BM) (**C**) after IA injection of 4T1-ERRα (**b**, **d**) compared to 4T1-CT (**a**, **c**) cells. Rank-positive osteoclasts were used as a positive control (see White arrow). Representative examples of three and two mice for FP tumor and BM, respectively. **D** Rank expression was barely detected by IHC in either 4T1-ERRα-LM (**b**, **d**) or 4T1-CT-LM (**a**, **c**). Representative example of $n = 2$. **E**, **F** Real-time RT-PCR was performed on triplicate samples and normalized against the ribosomal protein gene *L32* to evaluate (**E**) *Rank* expression in bone and lung metastases extracted from 4T1-ERRα versus 4T1-CT tumor-bearing animals ($n = 2$) (ANOVA: $P < 0.0001$, unpaired *t*-test $P = 0.0123$ for bone metastases) and (**F**) *Rankl* expression in total normal bone and lung (unpaired *t*-test $P = 0.0112$). **G** MCF7 clones overexpressing ERRα or ERRαAF2 were obtained after retroviral transfection. ERRα overexpression was assessed by Western blotting and compared to α-tubulin. **H** and **I** Real-time RT-PCR was performed on triplicate samples and normalized against the ribosomal protein gene *L32* to evaluate *RANK* expression in (**H**) MCF7 clones (ANOVA: $P = 0.0135$, unpaired *t*-test $P = 0.0041$) and (**I**) MDA-MD231-B02(B02) clones (ANOVA: $P = 0.0031$, unpaired *t*-test $P = 0.0032$). **J**–**M** C29 treatment induced a decrease in Rank expression in both parental 4T1 and MCF7 cells lines. **J**, **K** ERRα protein by Western blot (**J**) and *Rank* mRNA by real-time PCR (**K**) were inhibited by C29 at 1 μM after 48 h (unpaired *t*-test, $P = 0.0311$) in 4T1 cells. (**L**, **M**) Inhibition of ERRα protein (**L**) induced by C29 at 1 and 5 μM after 48 h in MCF7 cells is associated with a decrease of *RANK* mRNA expression (**M**) (ANOVA: $P = 0.0016$, unpaired *t*-test $P = 0.0127$ and $P = 0.0062$). (**N**) Real-time PCR was performed on triplicate samples to evaluate *ERRα* and *RANK* expression in the BC-M1 cells under low O_2 conditions compared with normoxia. *ERRα* and *RANK* expression was higher under low O_2 conditions (unpaired *t*-test $P = 0.0143$ and $P = 0.0016$ for *ERRα* and *RANK*, respectively). All in vitro assays were repeated at least two times. Data are plotted as mean ± SEM. Bar = 200 μm, T: Tumor, B: Bone

line and co-stimulated in BC-M1 cells cultured under low O_2 versus normoxia conditions (Fig. 3N) [31].

That *Rank* stimulation has functional consequences is supported by the observation that Rankl significantly stimulated migration of 4T1-ERRα cells (4T1-ERRα-versus-4T1-ERRα+Rankl) (Fig. 4A, B). Unexpectedly, the migratory ability of untreated 4T1-ERRα cells was lower than that of untreated 4T1-CT cells but this was reversed by Rankl treatment (Fig. 4B), revealing the high sensitivity of 4T1-ERRα cells to Rankl. Rankl had no effect on migration of 4T1-ERRαAF2 (4T1-ERRαAF2-versus−4T1-ERRαAF2 +Rankl) (Fig. 4C, D). Consistent with ERRα-Rank

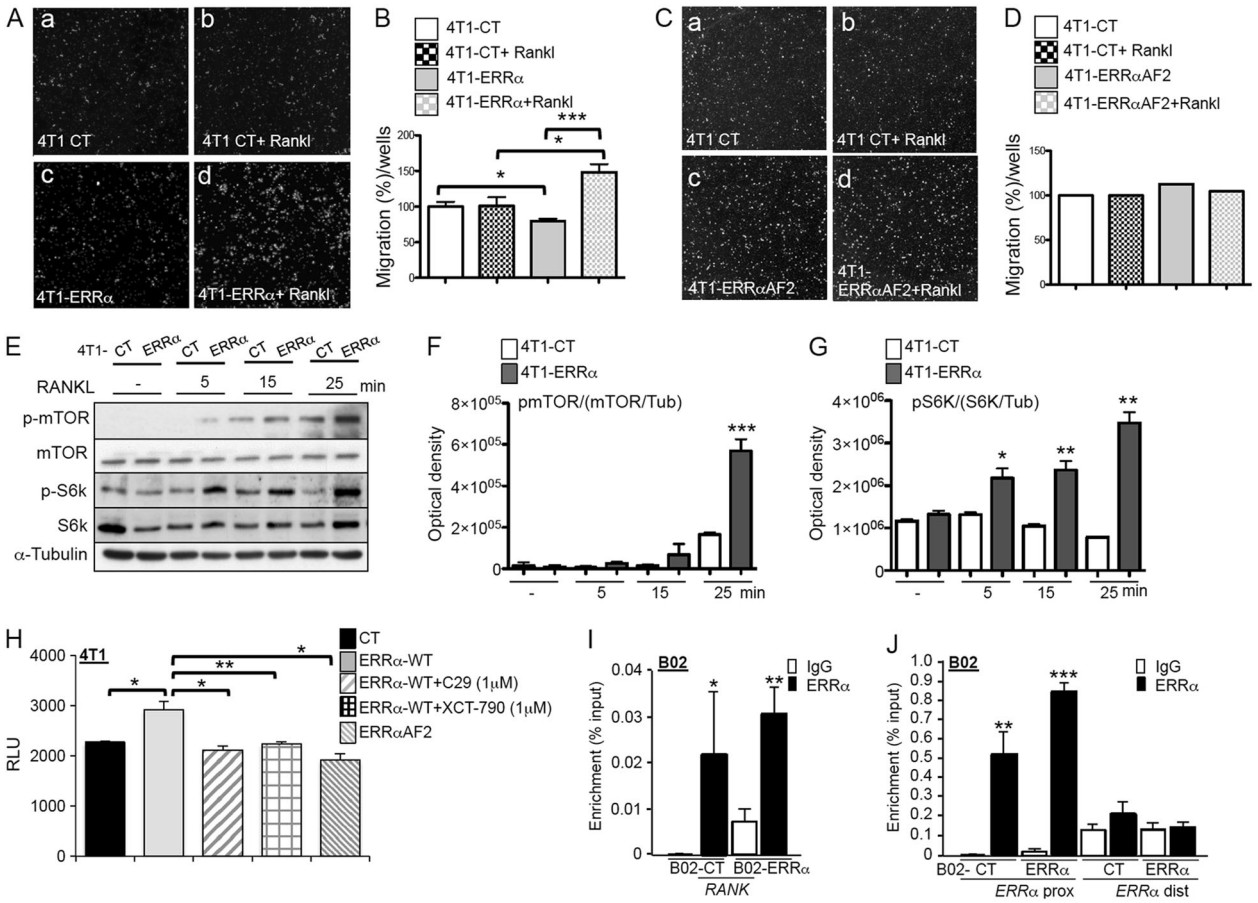

Fig. 4 Increased migration capacity of BCa cells overexpressing ERRα after Rankl treatment. **A**, **B** Migration was increased in 4T1-ERRα cells (clones 1–3) after Rankl treatment (50 ng/mL) for 12 h (4T1-ERRα *versus* 4T1-ERRα+Rankl: ANOVA: $P = 0.0005$, unpaired *t*-test $P = 0.0001$). The percentage of migration of 4T1-CT cells (clones 1–2) was unchanged after Rankl treatment (4T1-CT *versus* 4T1-CT +Rankl). In the absence of added RankL, migration of 4T1-ERRα cells was lower than that of 4T1-CT cells ($P = 0.0019$), but the opposite was observed after Rankl treatment ($P = 0.002$: 4T1-CT +Rankl *versus* 4T1-ERRα+Rankl). **C**, **D** Migration was not modulated in 4T1-ERRαAF2 cells (clones 1–3) after Rankl treatment (50 ng/mL) for 12 h (4T1-ERRαAF2 *versus* 4T1-ERRαAF2+Rankl). **E–G** Rankl signaling was assessed by treating 4T1-ERRα cells (clones1–3) and 4T1-CT cells (clones1–2) cells with RankL for different times (0, 5, 15, 25 min). Activation of mTOR and S6K was assessed with α-tubulin as loading control. mTOR and S6K were markedly activated in 4T1-ERRα cells at 5–25 min. **H** Reporter activity shows the activation of the Rank promoter activity by ERRα in 4T1 cells (CT *versus* ERRα-WT ANOVA: $P = 0.0004$, unpaired *t*-test $P = 0.0347$) that was blocked by C29 (1 μM) and XCT-790 (1 μM) and which is dependent on a functional ERRαAF2 domain (cf. ERRα-WT *versus* ERRα-WT +C29 or ERRα-WT+XCT790, or ERRαAF2) ($P = 0.00275$; $P = 0.0058$; and $P = 0.0022$, respectively). **I** ERRα binding to the human *RANK* locus was analyzed using ChIP-qPCR in control BO2-CT(CT) and BO2-ERRα (ERRα) cells (IgG *versus* ERRα in B02-CT ($P = 0.0237$) and in B02-ERRα ($P = 0.0015$)). **J** ERRα binding to a proximal (prox), but not to distal (dist) element of its own human promoter was used as positive (IgG *versus* ERRα in B02-CT ($P = 0.0023$) and in B02-ERRα ($P < 0.0001$)) and negative controls, respectively. Percent enrichments relative to input of a representative experiment are shown using anti-ERRα or non-specific rabbit-IgG antibody as a negative control. All in vitro assays were repeated two times. ChIP assay data are representative of two independant ChIP experiments. Data are plotted as mean ± SEM

signaling, mTOR/S6K phosphorylation was higher in Rankl-treated 4T1-ERRα cells (Fig. 4E–G) [27]. C29 and the XCT-790 [8] inhibited *Rank* mRNA expression in 4T1 parental cells after 24 h treatment and the endogenous ERRα activity decreased by C29 treatment (Supplementary Fig. S5AB) suggesting that the effect of ERRα on *Rank* expression is direct. This is supported by the finding that ERRα transactivates the *Rank* promoter in 4T1 cells (CT-versus-ERRαWT) and that this transactivation is dependent on a functional ERRαAF2 domain (ERRα-versus-ERRαWT ++C29, ERRαWT+XCT790 or ERRαAF2) (Fig. 4H). By using ChIP-qPCR in BO2-CT and BO2-ERRα cells, we also show ERRα binding on an ERRE site (TGAAGGTCA) localized on the human *RANK* locus (Fig. 4I) (Supplementary Fig. S5C) [20]. ERRα binding to a proximal (prox), but not to distal (dist) element of its own human promoter was used as positive and negative controls, respectively (Fig. 4J) [32, 33].

Pharmacological inhibition of ERRα reduces mammary tumor growth, bone marrow micro-metastases formation, and RANK expression in vivo

To determine whether inhibition of *ERR*α abrogates FP-tumor progression and BCa cell dissemination to bone, mice were inoculated with 4T1-ERRα cells and treated with the C29 or vehicle from the time of tumor appearance to tumor resection. Tumor weight/volume was reduced in 4T1-ERRα-FP tumor-bearing animals treated with C29 (Fig. 5A–C), as was TCB (Fig. 5D, E) but not LM (Supplementary Fig. S6E), without C29 toxicity (Supplementary Fig. S6A–D). *ERR*α and *Rank* mRNA and protein expression were reduced in FP-tumors in C29-treated mice (Fig. 5F) (Supplementary Fig. S7A,B).

Bioinformatics analysis reveals an extensive RANK–ESRRA regulatory interactome

To address further a RANK and ESRRA connection, we combined bioinformatics analyses of protein interaction networks and transcriptional regulator databases. We first built an extended network (Supplementary Fig. S8, Table S3) from public datasets and then defined a minimal network that included well-known ESRRA regulators, *e.g.* HDAC8, AIB1, SIRT1, SHP1, and linked ESRRA–RANK signaling, as exemplified by the presence of TRAFs and c-SRC (Fig. 5G) [34]. More than half (32 out of 62 proteins) of the regulators within the network are associated with extracellular matrix (ECM) regulation, cell adhesion and migration (see gray boxes, Fig. 5G) and a further half of these (16 of 32) are proteins encoded by genes that are potentially directly regulated by ESRRA (Fig. 5H, Supplementary Table S4). By shortest path analysis, we also identified two new potential ESRRA–RANK-associated regulators, such as MEX67 and SP1 (Fig. 5G).

ERRα/RANK are linked in BCa patients who developed BM

Meta-analysis of the GSE14020 dataset confirmed a positive association of *ERR*α and *RANK* in patients who developed BM but not in patients who developed lung and liver metastases (Table 2A) [35]. Moreover, in the Curie Institute cohort ($n = 446$), stratification of BCa patients into subtypes revealed a positive correlation between *ERR*α and *RANK* in Triple Negative patients (NNN) and Luminal BCa patients ($HR^{+}ERBB2$) but not ERBB2+patients (HR− and HR+) (Table 2B; Supplementary Fig. S9A,B; Table S5) [36]. Reinforcing our clinical data obtained in the NKI-294 cohort (Fig. 1D, E), Kaplan–Meier curves demonstrated that high *ERR*α expression is correlated with a decrease in BMFS but not LMFS in the Curie Institute cohort (Fig. 6A, B). No correlation was observed between *ERR*α and *RANKL* (*TNFSF11*) (Table 2B). Expression levels of *ERR*α and *RANK* were positively correlated in the TCGA dataset (Supplementary Fig. S9C) and in primary BCa samples (HR+ERBB2−) in combined microarray datasets (GSE12276-GSE2034-GSE2603)($n = 248$) (Table 2C; Supplementary Table S6). The strongest correlation was observed in patients who had developed only BM (Pearson $R = 0.5145$) and no correlation was observed in non-metastatic patients (No Mets).

ERRα is highly expressed in primary tumors from BRCA1-mutated carriers

Recently, *RANK/RANKL* were shown to control *BRCA1* mutation-driven mammary tumor formation and progressions [37], prompting us to ask whether *ERR*α and *BRCA1* expression is correlated. Using microarray datasets (GSE12276-GSE2034-GSE2603), we found a positive correlation between *ERR*α and *BRCA1* in BCa samples in patients who had developed both visceral+bone and only BM, and with *BRCA2* expression in patients with metastases at all sites (Table 2C). Since these datasets were not informative on the *BRCA1* and *2* mutations status, we used the METABRIC cohorts that include 2051 radically resected primary BCa, where $BRCA1^{mut}$ or 2^{mut} were identified. *ERR*α expression level was higher in $BRCA1^{mut}$ carriers but not $BRCA2^{mut}$-carriers compared to those with no mutations (Fig. 6C). By bioinformatics, our minimal network was structured over three main protein hubs (ESRRA, ESR, and BRCA1) (Fig. 5G). Systematic shortest path analysis revealed that ESRRA could control RANK and BRAC1 signaling (Fig. 6D) and, more specifically, BRCA1 through SRC1, AIB1, SP1, RIP140, and ESR which are ESRRA regulators [13, 14, 38, 39]. ESRRA may also directly regulate BRCA1 (with five potential ESRRA-binding sites) (Fig. 6F) and ESR, AIB1, SRC1, MEX67, and SP1 (Fig. 6F).

Discussion

Our findings indicate that *ERR*α is expressed in CTCs and promotes BCa cell homing to bone. The identification of *Rank* as an *ERR*α-regulated gene in our pre-clinical 4T1 cell model and *ERR*α/*RANK*-positive association in BCa patient cohorts provide new mechanistic insights into ERRα-regulated pathways mediating early BCa cell colonization of bone.

Elevated ERRα expression has been associated with tumor aggressiveness [13]. The fact that we have observed ERRα expression in CTCs of BCa metastatic patients and documented changes in BCa cell migration with changes

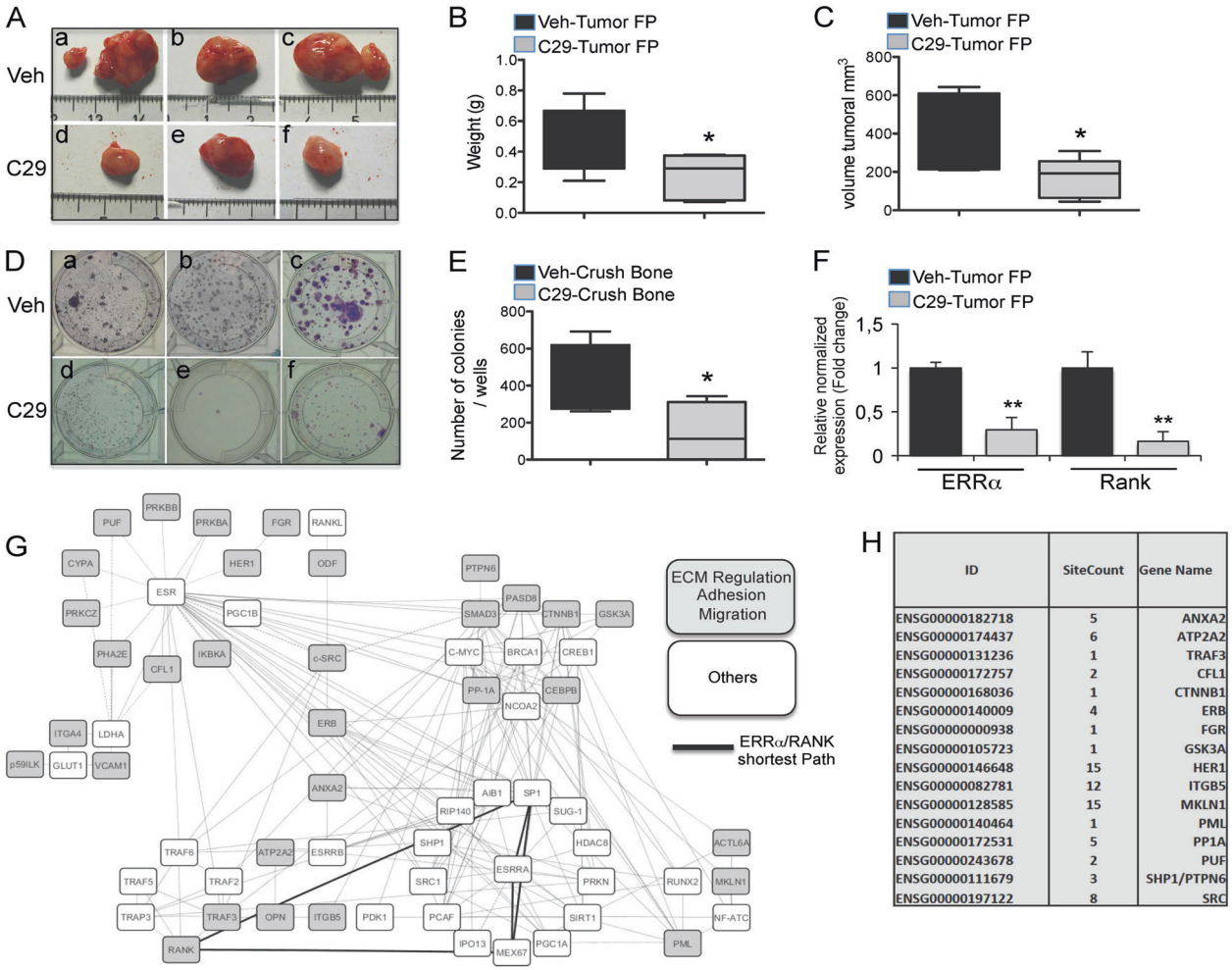

ID	SiteCount	Gene Name
ENSG00000182718	5	ANXA2
ENSG00000174437	6	ATP2A2
ENSG00000131236	1	TRAF3
ENSG00000172757	2	CFL1
ENSG00000168036	1	CTNNB1
ENSG00000140009	4	ERB
ENSG00000000938	1	FGR
ENSG00000105723	1	GSK3A
ENSG00000146648	15	HER1
ENSG00000082781	12	ITGB5
ENSG00000128585	15	MKLN1
ENSG00000140464	1	PML
ENSG00000172531	5	PP1A
ENSG00000243678	2	PUF
ENSG00000111679	3	SHP1/PTPN6
ENSG00000197122	8	SRC

Fig. 5 Pharmacological inhibition of ERRα. **A** 4T1-ERRα (clones 1–3) cells were inoculated into the FP of the mammary gland of BALB/c mice and mice were treated with C29 (10 mg/kg) for 10 days from the time of tumor appearance to tumor resection (day 14). C29 (C29-Tumor-FP) (**d–f**) decreased tumor expansion compared to tumor growth in vehicle treated mice (**a–c**). **B**, **C** Weight and volume of tumors dissected at endpoint ($n = 9$, unpaired *t*-test, weight: $P = 0.014$; Mann and Whitney: volume: $P = 0.019$). **D**, **E** After tumor resection, animals were kept for an additional 21 days, bones were then crushed and released cells were cultured for 3 weeks. C29 treatment (**Dd–f**; **E**) decreased TCB number compared Veh (**Da–c**; **E**) ($n = 5$, 142 ± 138 *versus* 416 ± 138, unpaired *t*-test, $P = 0.035$). **F** Real-time PCR performed on RNA extracted from C29 (C29-Tumor-FP) *versus* vehicle-treated (Veh-Tumor-FP) mice ($n = 3$, unpaired *t*-test $P = 0.004$ for *ERRα* and $P = 0.0032$ for *Rank*) confirmed a decrease in the expression of *ERRα* and *Rank* in treated animals. **G** By bioinformatics analysis, a protein interaction and transcriptional regulation network was built. Potential new regulators, including MEX67 and SP1, were identified through systematic shortest path definition of cross-talks (see black bold line). 32 out of 62 regulatory proteins are associated with ECM regulation, cell adhesion and migration (see gray boxes). **H** GTRD database analysis indicated that 16 of the 32 regulatory proteins are encoded by genes that could be directly regulated by ESRRA

in ERRα activity strengthens the notion that ERRα may be involved into CTCs survival and metastases.

We found that a high level of ERRα was associated with bone but not LM in our mouse experimental model of spontaneous metastatic BCa and in two independent ($n =$ 740) BCa patient cohorts, suggesting that ERRα/RANK expression in primary tumors may be a predictive marker of BM occurrence in BCa patients. With respect to bone colonization, our identification of *RANK* as a new *ERRα*-regulated gene is notable. RANK, the cognate receptor of RANKL, was described as being predictive of poor prognosis in patients with BM but not in patients with visceral metastases [28, 29, 40]. One explanation comes from evidence that RANKL is a chemoattractant that is more highly expressed in bone than lung, thus promoting bone colonization (Fig. 3F): RANKL produced by osteoblasts has been shown to attract RANK-expressing cancer cells and induce their migration in the bone microenvironment [41]. This mechanism has been observed not only in BCa but also in other cancers [29] indicating that RANKL is one of the important "soil" factors that promote BCa-Rank+cell bone colonization. Additionally, knockdown of *Rank* expression in metastatic BCa-reduced BM indicating that RANK is required for BCa migratory response toward RANKL-

Table 2 Correlation between ERRα and Rank expression in BCa patients

A				
GSE14020 $n = 65$	All ESRRA 65	Bone Mets ESRRA 18	Lung Mets ESRRA 20	Liver Mets ESRRA 5
Pearson-correlation coefficient				
TNFRSF11A (RANK)	$R = 0.510$	$R = 0.515$	$R = 0.457$	$R = 0.009$
	P < 0.0001	***P = 0.0287***	$P = 0.0504$(NS)	*P = 0.884(NS)*

B					
Curie $n = 446$	All ESRRA 446	NNN ESRRA 68	HR-ERBB2 +ESRRA 42	HR+ERBB2- ESRRA 285	HR+ERBB2 +ESRRA 51
Spearman-correlation coefficient					
TNFRSF11A (RANK)	$R = 0.318$	$R = 0.299$	$R = 0.25$	$R = 0.303$	$R = 0.203$
	P < 0.0000001	***P = 0.013***	*P = 0.11(NS)*	***P = 0.00000099***	$P = 0.15$(NS)
TNFSF11 (RANKL)	$R = 0.054$	$R = 0.146$	$R = 0.058$	$R = -0.001$	$R = -0.017$
	P = 0.25(NS)	*P = 0.23 (NS)*	*P = 0.71(NS)*	*P = 0.99(NS)*	*P = 0.90(NS)*

C				
GSE12276 2034-2603 $n = 248$	All ESRRA 248	No Mets ESRRA 121	Visceral +bone ESRRA 53	Bone only ESRRA 74
Pearson-correlation coefficient				
TNFRSF11A (RANK)	$R = 0.4063$	$R = 0.1050$	$R = 0.4667$	$R = 0.5145$
	P < 0.0001	*P = 0.2517(NS)*	***P = 0.0005***	***P < 0.0001***
BRCA1	$R = 0.2949$	$R = 0.1470$	$R = 0.332$	$R = 0.2846$
	P < 0.0001	*P = 0.1075(NS)*	***P = 0.0152***	***P = 0.0140***
BRCA2	$R = 0.5113$	$R = 0.3559$	$R = 0.425$	$R = 0.5026$
	P < 0.0001	***P*** < 0.0001	***P*** $= 0.0015$	***P < 0.0001***

A Meta-analysis of the public dataset GSE14020 ($n = 65$) revealed correlation between *ERR*α and *RANK* in all tumors and in patients with bone but not lung or liver metastases. **B** Meta-analysis of the Curie BCa cohorts ($n = 446$) revealed correlation between *ERR*α and *RANK (TNFRSF11A)* mRNA expression in the total tumor population, in the triple negative group and in the luminal group (HR+ERBB2−). No correlation was found in ERBB2+patients (HR− and HR+) or with *RANKL* (*TNFSF11*). **C** Meta-analysis of public datasets (GSE12276, GSE2034, and GSE2603) ($n = 248$) revealed correlation between *ERR*α and *RANK, BRCA1* and *BRCA2* expression levels in all tumors, in patients with visceral and bone metastases or only bone metastases. Correlation scores were calculated using the Spearman correlation coefficient for the Curie cohort and the Pearson correlation coefficient for GSE14020 and GSE12276-GSE2034-GSE2603. *P*-values < 0.05 were considered statistically significant

expressing bone cells in vivo [41, 42]. This, together with the fact that the 4T1-CT cells that colonized bone highly express *Rank* while *Rank* was barely detectable in lung (Fig. 3Ca, Da), strongly suggests that RANK is a prerequisite factor for cancer cell colonization of bone. Consistent with RANK–RANKL signaling [27], EMT, mTOR/S6K, and cell migration were stimulated in 4T1-ERRα.

RANKL has recently been linked to mitochondrial mass in osteoclasts [17, 43], and glucose uptake and glycolysis with increased PGC1α, GLUT1, LDHA, and VEGF expression in osteoblasts resembling the Warburg effect [44, 45]. *ERR*α and *Pgc1*α, which is up-regulated in 4T1-ERRα-FP, are known to play a major role in coordinating oncometabolic programs [13]. Interestingly, these genes which are all direct targets of ERRα, were all up-regulated in vivo in 4T1-ERRα-FP, suggesting that RANKL–RANK may also participate in cancer cell metabolic reprogramming to meet the rapid energy requirement for survival and metastases. Interestingly, by bioinformatic, we identified MEX67 and SP1 two potential ESRRA-RANK-associated

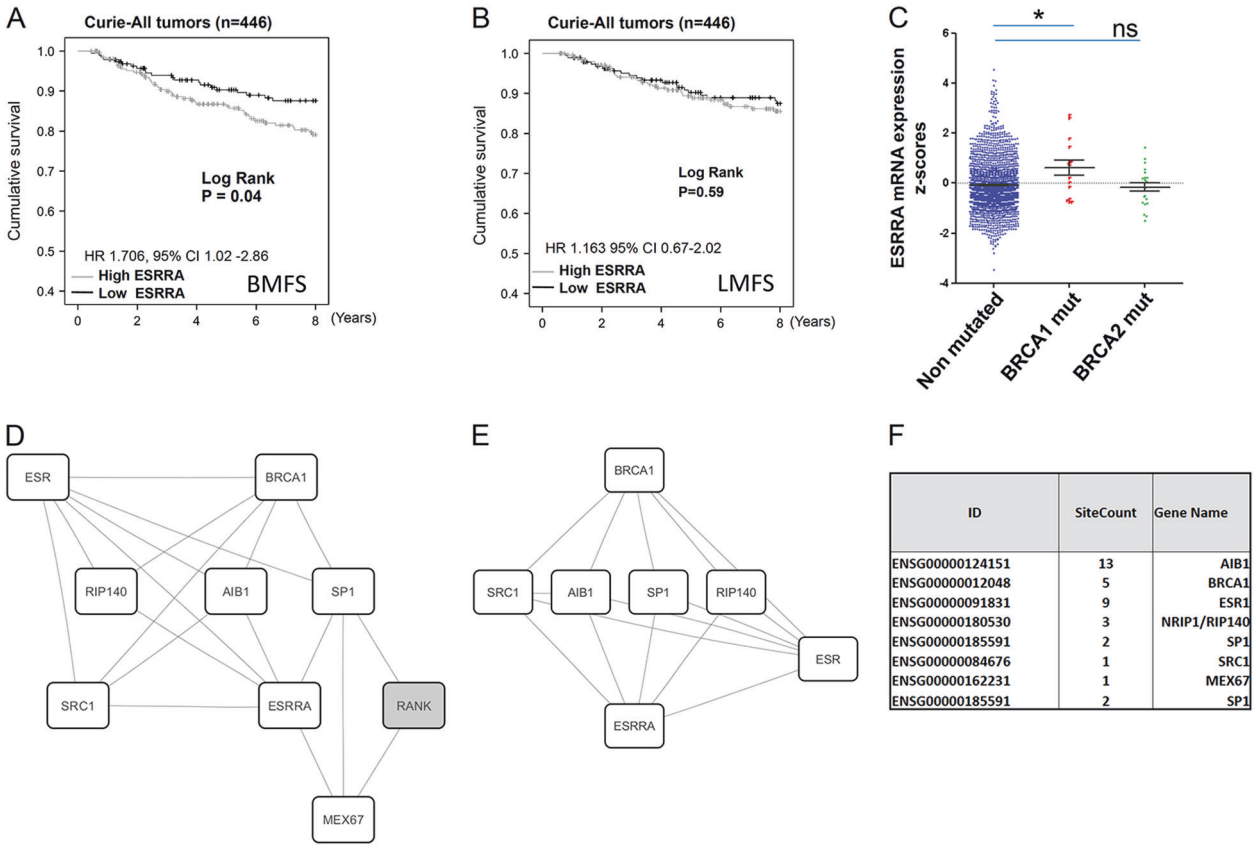

Fig. 6 **A** Kaplan–Meier curves constructed after segmentation into two groups on the basis of the median value for ERRα expression show correlation between high expression of ERRα and lower bone metastases-free survival (BMFS) in Curie BCa cohorts ($n = 446$, $P = 0.04$); Low ≤ 50% quartile; high ≥ 50%. **B** No correlation was found between high expression of ERRα and lung metastases free-survival (LMFS). **C** Meta-analysis of the METABRIC cohorts that include 2051 radically resected primary BCa, where BRCA1 and 2 mutations were identified, revealed correlation between high *ERR*α and BRCA1 mutation (Mann–Whitney $P = 0.02$). No link was found between ERRα expression and BRCA2 mutation. **D** Analysis of our minimal network (Fig. 5G) showed that ESRRA could control RANK and BRAC1 signaling and, more specifically, (**E**) BRCA1 through SRC1, AIB1, SP1, RIP140 and ESR. (**F**) GTRD database analysis indicated that ESRRA may directly regulate BRCA1; ESRRA-binding sites are also present in ESR, AIB1, SRC1, MEX67, and SP1

regulators that had been detected in invasive ductal BCa and as an ERRα transcription control factor-coregulator, respectively [46, 47] (Expression-Atlas-EMBL—EBI). Moreover, the RANK/RANKL axis is a critical regulator of BRCA1-mutation-driven BCa and anti-RANKL therapy is now proposed as a preventive strategy for women carrying BRCA1 mutations [37, 48]. We found a significant correlation between high ERRα and BRCA1^{mut} in BRCA1^{mut} carriers, implying that ERRα may participate directly in the RANKL/RANK control of progenitor cell expansion and tumorigenesis in inherited BCa and/or via the modulation of BRCA1 (by, *e.g.*, the ERRα coregulators, SRC-1, AIB1, and RIP140) (Fig. 6D–F). The presence of ESR in our shortest path analysis also reinforces the link between ERRα/ERα in BCa. Similarly to the suggestion that inhibition of the RANKL/RANK axis may be a therapeutic target for BRCA1^{mut} carriers, inhibition of an upstream RANK regulator, ERRα, may also constitute a useful new therapeutic approach for these patients. In conclusion, we report for the first time a RANK/ERRα axis in BCa that contributes new mechanistic understanding of the negative outcome associated with ERRα in BCa.

Materials and methods

Ethics approval

BALB/c female mice were purchased from Janvier and handled according to the French Ministerial Decree no. 87–848 of 19 October 1987. Experimental protocols were approved by the Institutional Animal Care and Use Committee at the Université-Lyon1 (France)(CEEA-55 Comité d'Ethique en Expérimentation Animale-DR2014-44-DR2015-28). Studies involving human primary specimens were carried out according to the principles embodied in the Declaration of Helsinki.

Study on BCa patient primary tumor specimens

Immunohistochemistry (IHC) was performed on formalin-fixed paraffin-embedded (FFPE) tumor tissue sections ($n = 100$) from the Austrian-Breast and Colorectal-Cancer-Study Group (ABCSG) Trial-6 [22]. For IHC, FFPE tumor tissue and a mouse monoclonal anti-ERRα antibody (1/50) (sc-65715, Santa-Cruz) were used. Sections were incubated with HRP-conjugated anti-mouse (Dako), stained using 3,3′-diaminobenzidine (Dako) and Mayer's hematoxylin (Merck). ERRα immunostaining was assessed by the *H*-score method [49].

Samples of 446 unilateral invasive primary breast tumors excised from women managed at Institut-Curie-Hôpital-René-Huguenin (France) for which grading information was available (Supplementary Table S5) were analyzed [36, 50]. The mean age of the patients was 61.8 years, and the median follow-up was 103.1 months. Since 2007, patients have signed inform consent. This study was approved by the review board and ethics committee of the institute. A tumor sample was considered suitable for our study if the proportion of tumor cells exceeded 70% [36]. Real-time-PCR was performed using specific primers (Supplementary Table S7) for human housekeeping gene *TBP* (TATA-box-binding protein), *ERR*α, *RANK*, and *RANKL* (ABI-Prism-7900 sequence-detection-system) (Perkin-Elmer-Applied-Biosystems, CA), and the PE-Biosystems analysis software according to the manufacturer's manuals [36]. Results were expressed as fold differences equal to $2^{-\Delta\Delta Ct}$.

Detection of ERRα in CTC

For ERRα detection in CTC detection, patients after signed inform consent, were recruited at the Cancer Institute of Montpellier in 2017 (Bioethic-committee D-RCB 2015-A00119-40). We first performed experiments by adding 200 BCa cells (SKBR3 and MDA-MB-231) to 7.5 mL of PBS. To mimic blood of BCa patients, we spiked 200 BCa cells in 7.5 mL of blood from healthy donors. Tumor cells were detected by using the CellSearch® system (Silicon-Biosystem, Menarini) with the CellSearch CTC Kit. This FDA-cleared semiautomatic system contains a ferrofluid-based capture reagent targeting all EpCAM-positive cells, which could be further identified as CTCs by a pan-keratin (CK8-18-19) and nuclear staining. Contaminating leukocytes were excluded by CD45 staining. For ERRα detection, we used the fourth channel of the CellSearch® and the anti-human ERRα/NR3B1-A488-conjugated polyclonal antibody (Novus, USA) (25 µg/mL). The corresponding Rabbit IgG-Isotype control (Alexa-Fluor®488) (Novus) was used at the same final concentration. Blood of three metastatic BCa patients were analyzed for the presence of CTCs over-expressing ERRα.

Meta-analysis of ESSRA expression

For the BCa cohorts "NKI" ($n = 295$) [23] and "METABRIC" ($n = 2051$) [51], the genomic and transcriptomic data were obtained through the cBioPortal Web resource (http://cbioportal.org). All statistical calculations were performed using PASW Statistics (version 18.0; SPSS Inc., Chicago, IL) and a two-sided unpaired Student's *t*-test. By using of the receiver operating characteristic method, we determine whether *ESRRA, ESRRB*, and *ESRRG* expression levels were able to define low-metastases and high-metastases risk populations.

For correlation analysis, published datasets were downloaded from the Gene-Expression-Omnibus including primary tumors, bone, lung, and liver metastases (GSE14020) ($n = 65$) [35] and primary tumor, no-metastases, visceral +bone or only BM (GSE12276-GSE2034-GSE2603) ($n = 248$) [52–54]. *Z*-scores were obtained by normalizing data were $\log_2$ transformed and calculating by subtracting the population mean from individual expression values for each gene and then dividing the difference by the population standard deviation. Correlation scores were calculated using the Pearson-correlation-coefficient. *P*-values < 0.05 were considered statistically significant. Statistical significance was determined by GraphPad Prism v5.02 using the two-sided Student's *t*-test.

Cell lines, transfection, and immunoblotting

Human MCF7 (year 2012) and mouse 4T1(year 2012) BCa cell lines were obtained from the American Type Culture Collection. 4T1, MDA-MB231-B02 [20] and MCF7 were cultured in DMEM or RPMI-1640 (Life-Technologies) medium, respectively, supplemented with 10% fetal bovine serum (FBS, Perbio) and 1% penicillin/streptomycin (Invitrogen) at 37 °C in a 5% CO_2 incubator. The human BC-M1 (Vimentin/CK5-positive, CK8/18-negative, HER2) cell line (generous gift from the Dr. K. Pantel lab) was obtained from a bone marrow aspirate of a BCa patient with no clinical signs of distant metastases at the time of the primary tumor resection [31, 55]. BC-M1 cells were cultured in complete RPMI-1640 medium (Life-Technologies) supplemented with 10% FBS, 200 U/mL penicillin/streptomycin (Life-Technologies), insulin–selenium–transferrin (IST) (Gibco, France), 50 ng/mL of epidermal growth factor (EGF), and 10 ng/mL of human basic-fibroblasts growth factor (bFGF) (Miltenyi-Biotec, France) at 37 °C in a 5% CO_2, low (10% of O_2), or normoxic (21% of O_2) conditions. Total mRNA was extracted using the RNAeasy Mini Kit (Qiagen, Courtabeuf).

Murine and human ERRα cDNA (ERRα) and the dominant-negative co-activator domain AF2 (AF2) mutant were obtained previously [20, 21, 56]. pSRα-ERRαWT and

pSRα-ERRαAF2 or empty vector constructs were transfected into parental 4T1 cells and cultured for 4 weeks in puromycin (2 µg/mL) (Life-Technologies). For MCF7 clones, a mix containing 1.5 µg Retroviral pLPCX-HumanERRαWT, pLPCX-HumanERRαAF2, or empty vector and 0.5 µg pCMV-VSV-G envelope vector (Cell-Biolabs) were transfected by calcium phosphate precipitation (CalPhos-mammalian-Transfection-Kit,Clontech), according to the manufacturer's instruction with selection in puromycin (2 µg/mL) (Life-Technologies) for 3 weeks.

Parental 4T1 and MCF7 cells were treated with the ERRα inverse-agonist C29 (AGVdiscovery, France) at 1 and 1–5 µM, respectively, for 24 and 48 h [9, 30, 33, 57]. XCT790 (Sigma) was also used at 1 µM [8]. DMSO was used as vehicle. For Rankl studies, 4T1-CT (two clones), 4T1-ERRα (three clones) were plated at 5×10^5 cells/well in complete medium. The next day, cells were starved for 24 h and then treated with Rankl (50 ng/mL) (R&D) for different times (0–5–15–25 min). Protein extraction and immunoblotting was performed as described [20], using antibodies against ERRα (Abcam-EPR46Y) (1:400), mTOR and pmTOR (Ser2481) (Cell-Signaling) (1:1000), S6K and pS6K (Thr389) (Cell-Signaling) (1:1000), or α-tubulin (Cell-Signaling) (1:1000) as protein-loading control [20, 21]. The experiments were done in triplicated and repeated two times.

Animal studies

BALB/c female mice (6 weeks), were housed in barrier conditions under isolated laminar flow hoods. Mice bearing tumor xenografts were monitored for established signs of distress and were humanely euthanized. Tumor fat pad (FP) experiments were performed ($n = 10$ for each groups) using the 4T1-CT (two clones), 4T1-ERRα (three clones), or 4T1-AF2 (three clones) cell lines (10^5 cells in 10 µL of PBS) injected into FP of the fourth mammary gland of mice as described [58]. Briefly, primary tumors were resected 2 weeks after cell injection and tumor weight and size were measured. For spontaneous metastases dissemination studies (lungs (macro-metastases), bone (micro-metastases)), mice were followed after resection for an additional 3 weeks at which time they were sacrificed. Lungs were collected for histological analysis or crushed (C29 experiment). Hind limbs were removed and crushed. Cells released from lungs (C29 experiment) and bone were incubated at 37 °C in the presence of DMEM supplemented with FBS and 6-Thioguanine (10 µg/mL) for 3 weeks before tumor cells that colonized the bone (TCB) and lung colonies were stained by using Crystal Violet and counted.

FP experiments were performed using 4T1-ERRα cells (three clones) (10^5 cells in 10 µL of PBS). When primary tumors reached ~30 mm^3, mice were randomized ($n = 10$), treated every 2 days for 10 days by intra-peritoneal injection with vehicle (DMSO 10%, 30% PEG) or C29 (10 mg/kg) [9, 57], then prepared and analyzed as above. Bone lesion experiments were performed using 4T1-CT (two clones) and 4T1-ERRα cells (three clones) cells (10^5 cells in 100 µL of PBS) injected intra-arterially (IA). After 2 weeks, bones and lungs were collected for histological analysis ($n = 2$). Some hind limbs and lungs were removed and crushed for mRNA extraction.

IHC on mice FP-tumor sections

5 µm paraffin sections were incubated overnight with RANK(1/50)(Abcam-64C1385), or Vegf-a(1/50)(Abcam-EP1176Y) or ERRα antibody (1/50)(Santa-Cruz-V19) [20], followed by incubation with horseradish peroxidase (HRP)-conjugated anti-mouse or anti-rabbit (Dako) antibodies for 1 h and staining with 3,3′-diaminobenzidine (Dako) and Mayer's hematoxylin (Merck).

Cell migration assay

Migration assays were done with the HTS FluoroBlok™-Multiwell-Insert-system (8 µm corning) as described [20]. After 12 h of starvation, 4T1-CT (two clones), 4T1-ERRα (three clones), and 4T1-ERRαAF2 (three clones)(5×10^4 cells) were plated in the upper chambers and the chemoattractant (0.5%FBS) with or without Rankl (50 ng/mL) (R&D) in the lower chambers. After 12 h at 37 °C in 5% CO_2 incubator, cells that had migrated through the filters were fixed, stained with DAPI (Life-Technologies) and counted. All experiments ($n = 2$) were run in triplicate, migration was expressed in % of migration/wells.

Transactivation assay

4T1 cells (10^6 cells/well in six-well plates) were transfected with a mouse Rank promoter-driven *Gaussia*-Luciferase-reporter plasmid (pEZX-PG04 RankLuc:−1450/+31) (Genecopoeia) and TurboFect Transfection Reagent according to the reverse transfection protocol (Thermo-Scientific). 4T1 cells were cotransfected with plasmids expressing ERRα-WT or mutated ERRαAF2. The ratio of DNA/Turbofect was 4 µg/6 µL. After overnight incubation, transfection medium was replaced with fresh medium containing DMSO 0.1% or XCT790(1 µM) or C29(1 µM). Medium aliquots were withdrawn at 48 h for measuring Gaussia Luciferase with the Secrete-Pair™ *Gaussia* Luciferase-Assay Kit in Buffer GL-S (Genecopoeia). The experiments were done in triplicated and repeated two times.

Real time-PCR

Total RNA was extracted with Trizol-reagent (Life-Technologies) and 2 µg was reverse-transcribed using SuperscriptTM-II (Life-Technologies) [21]. Real-time PCR was performed on a Mastercycler-ep-Realplex (Eppendorf) with primers specific to human and mouse genes (Supplementary Table S7) using Quantifast-SYBR-Green (Life-Technologies) according to the manufacturer's instructions [21]. The ribosomal protein L32 gene was used as control and relative results expressed as fold differences equal to $2^{-\Delta\Delta Ct}$.

Protein–Protein interaction network reconstruction and analysis

We reconstructed the protein–protein interaction network with BIOGRID (release 3.4.160) protein–protein interaction data from *Homo sapiens* with Proteomics-Standard-Initiative-Common-QUery-InterfaCe (PSICQUIC) retrieval (05292018) and CytoScape environment [34]. A custom approach was used to define a protein interactome of the following proteins: ESRRA-ESR-RIP140-SRC1-SRC2-SRC3-PGC1A-PGC1B-TRAF6-TRAF5-TRAF2-PDK1-GLUT1-LDHA-TNFRSF11A. The resulting interactome encompasses more than 300 proteins (so called "Extended Network"). To determine the connectors between ESR, RANK, BRCA1, and ESRRA, a custom approach combining shortest path and connectivity degree analysis was applied to determine a "Minimal Network" acknowledging connections that may support ESRRA signaling. We overlaid information from Gene-Ontology-consortium to pinpoint proteins that are already known to be involved in the regulation of ECM assembly and degradation, as well as cellular adhesion and migration (GO-IDs: 1903053-0022617-012715-0007155-0016477). Generated network maps by using CyNetShare (cynetshare.ucsd.edu) can be up-loaded for public access (https://doi.org/10.18119/N9PC7F) (Supplementary Fig. S8) [59].

Determination of ESRRA-mediated transcriptional regulation

We determined the proteins encoded by human genes under the control of ESRRA and the number of regulatory sites within these genes using the GTRD ChIP-seq database (http://gtrd.biouml.org/) [60].

Chromatine immunoprecipitation (ChIP)

ChIP assays were performed as previously described [61] from MDA-MB231-B02-CT and -ERRα cells [20] using either a monoclonal rabbit anti-ERRα (13826) (Cell-Signaling) or a control rabbit IgG(2729) antibody (Cell-Signaling). The immune-precipitated genomic DNA was purified using NucleoSpin Clean-up colums (Macherey-Nagel, Germany) and analyzed by qPCR. Quantification of ChIP enrichment was calculated relative to input values. Distal and proximal elements of ERRα gene were used as negative and positive controls, respectively (Supplementary Table S7) [32, 33].

Statistical analysis

Statistical analysis was performed using GraphPad Prism software (San Diego, USA). Data were analyzed statistically by the non-parametric Mann–Whitney *U*-test or unpaired *t*-test for in vivo studies ($n = 10$ mice for each group (bioStaTGV), unblinding studies). In vitro assays were repeated at least two times and performed on triplicate samples. Data were analyzed using ANOVA and Student's *t*-test to assess the differences between groups. MFS, LMFS, and BMFS were determined as the interval between diagnosis and detection of the first metastases. Survival distributions were estimated by the Kaplan–Meier method, and the significance of differences between survival rates was ascertained using the log-rank test. Univariate and multivariable analyses using Cox proportional hazards models were used to assess the independent contribution of each variable to organ-specific MFS. All data are presented as means ± SEM with variance were similar between the groups. Statistical tests, differences were considered significant at confidence levels >95% ($p < 0.05$).

Acknowledgements The authors thank Anne Flourens, Cyprien Tilmant, Tina Louadj, and both CeCIL and ALECS platforms (Faculté de Médecine Laennec, Lyon) for their assistance.

Funding This work was supported by the National Center for Scientific Research (CNRS) to EB, the National Institute of Health and Medical Research (INSERM), the University of Lyon1, La Ligue Nationale (Drôme), Inserm-Transfert (EB). GV was supported by the Labex DEVweCAN, MG, MB by the French National Cancer Institute (INCa), CK by the Marie-Curie-Individual-Fellowship (655777-miR-OMeS). CAP, LC, and MM by CANCER-ID (FP7/2007-2013) and EFPIA.

Compliance with ethical standards

Conflict of interest The authors declare that they have no conflict of interest.

References

1. Lambert A, Pattabiraman D, Weinberg R. Emerging biological principles of metastasis. Cell. 2017;168:670–91.
2. Kan C, Vargas G, Pape F, Clézardin P. Cancer cell colonisation in the bone microenvironment. Int J Mol Sci. 2016;17:E1674.

3. Brodowicz T, Hadji P, Niepel D, Diel I. Early identification and intervention matters: a comprehensive review of current evidence and recommendations for the monitoring of bone health in patients with cancer. Cancer Treat Rev. 2017;61:23–34.
4. D'Oronzo S, Brown J, Coleman R. The role of biomarkers in the management of bone-homing malignancies. JBone Oncol. 2017;9:1–9.
5. Lacey D, Boyle W, Simonet W, Kostenuik P, Dougall W, Sullivan J, et al. Bench to bedside: elucidation of the OPG-RANK-RANKL pathway and the development of denosumab. Nat Rev Drug Discov. 2012;11:401–19.
6. Benoit G, Cooney A, Giguere V, Ingraham H, Lazar M, Muscat G, et al. International Union of Pharmacology. LXVI. Orphan nuclear receptors. Pharmacol Rev. 2006;58:798–836.
7. Giguere V, Yang N, Segui P, Evans RM. Identification of a new class of steroid hormone receptors. Nature. 1988;331:91–4.
8. Willy PJ, Murray IR, Qian J, Busch BB, Stevens WC Jr, Martin R, et al. Regulation of PPARgamma coactivator 1alpha (PGC-1alpha) signaling by an estrogen-related receptor alpha (ERRalpha) ligand. Proc Natl Acad Sci USA. 2004;101:8912–7.
9. Patch RJ, Searle LL, Kim AJ, De D, Zhu X, Askari HB, et al. Identification of diaryl ether-based ligands for estrogen-related receptor alpha as potential antidiabetic agents. J Med Chem. 2011;54:788–808.
10. Audet-Walsh E, Giguére V. The multiple universes of estrogen-related receptor α and γ in metabolic control and related diseases. Acta Pharmacol Sin. 2015;36:51–61.
11. Ariazi EA, Clark GM, Mertz JE. Estrogen-related receptor alpha and estrogen-related receptor gamma associate with unfavorable and favorable biomarkers, respectively, in human breast cancer. Cancer Res. 2002;62:6510–8.
12. Wu D, Cheung A, Wang Y, Yu S, Chan F. The emerging roles of orphan nuclear receptors in prostate cancer. Biochim Biophys Acta. 2016;1866:23–36.
13. Tam I, Giguère G. There and back again: the journey of the estrogen-related receptors in the cancer realm. J Steroid Biochem Mol Biol. 2016;157:13–9.
14. Deblois GGV. Oestrogen-related receptors in breast cancer: control of cellular metabolism and beyond. Nat Rev Cancer. 2013;13:27–36.
15. Dwyer MA, Joseph JD, Wade HE, Eaton ML, Kunder RS, Kazmin D, et al. WNT11 expression is induced by estrogen-related receptor alpha and beta-catenin and acts in an autocrine manner to increase cancer cell migration. Cancer Res. 2010;70:9298–308.
16. Bonnelye E, Aubin JE. An energetic orphan in an endocrine tissue: a revised perspective of the function of estrogen receptor-related receptor alpha in bone and cartilage. J Bone Miner Res. 2013;28:225–33.
17. Bae S, Lee M, Mun S, Giannopoulou E, Yong-Gonzalez V, Cross J, et al. MYC-dependent oxidative metabolism regulates osteoclastogenesis via nuclear receptor ERRα. J Clin Invest. 2017;127:2555–68.
18. Delhon I, Gutzwiller S, Morvan F, Rangwala S, Wyder L, Evans G, et al. Absence of estrogen receptor-related-alpha increases osteoblastic differentiation and cancellous bone mineral density. Endocrinology. 2009;150:4463–72.
19. Wei WWX, Yang M, Smith LC, Dechow PC, Sonoda J, Evans RM, et al. PGC1beta mediates PPARgamma activation of osteoclastogenesis and rosiglitazone-induced bone loss. Cell Metab. 2010;11:503–16.
20. Fradet A, Sorel H, Bouazza L, Goehrig D, Depalle B, Bellahcene A, et al. Dual function of ERRalpha in breast cancer and bone metastasis formation: implication of VEGF and osteoprotegerin. Cancer Res. 2011;71:5728–38.
21. Fradet A, Bouchet M, Delliaux C, Gervais G, Kan C, Benetollo C, et al. Estrogen related receptor alpha in castration-resistant prostate cancer cells promotes tumor progression in bone. Oncotarget. 2016;7:77071–86.
22. Schmid M, Jakesz R, Samonigg H, Kubista E, Gnant M, Menzel C, et al. Randomized trial of tamoxifen versus tamoxifen plus aminoglutethimide as adjuvant treatment in postmenopausal breast cancer patients with hormone receptor-positive disease: Austrian breast and colorectal cancer study group trial 6. J Clin Oncol. 2003;21:984–90.
23. van de Vijver M, He Y, van't Veer L, Dai H, Hart A, Voskuil D, et al. A gene-expression signature as a predictor of survival in breast cancer. N Engl J Med. 2002;19:1999–2009.
24. Souza Garcia C, Rios de Araujo M, Paz Lopes M, Ferreira M, Dantas Cassali G. Morphological and immunophenotipical characterization of murine mammary carcinoma 4t1. Braz J Vet Pathol. 2014;7:158–65.
25. Aslakson CJ, Miller FR. Selective events in the metastatic process defined by analysis of the sequential dissemination of subpopulations of a mouse mammary tumor. Cancer Res. 1992;52:1399–405.
26. Stein RA, Gaillard S, McDonnell DP. Estrogen-related receptor alpha induces the expression of vascular endothelial growth factor in breast cancer cells. J Steroid Biochem Mol Biol. 2009;114:106–12.
27. Boyle WJ, Simonet WS, Lacey DL. Osteoclast differentiation and activation. Nature. 2003;423:337–42.
28. Santini D, Schiavon G, Vincenzi B, Gaeta L, Pantano F, Russo A, et al. Receptor activator of NF-kB (RANK) expression in primary tumors associates with bone metastasis occurrence in breast cancer patients. PLoS One. 2011;6:e19234.
29. Jones DH, Nakashima T, Sanchez OH, Kozieradzki I, Komarova SV, Sarosi I, et al. Regulation of cancer cell migration and bone metastasis by RANKL. Nature. 2006;440:692–6.
30. Hong E, Levasseur M, Dufour C, Perry M, Giguère V. Loss of estrogen-related receptor α promotes hepatocarcinogenesis development via metabolic and inflammatory disturbances. Proc Natl Acad Sci USA. 2013;110:17975–80.
31. Bartkowiak K, Kwiatkowski M, Buck F, Gorges T, Nilse L, Assmann V, et al. Disseminated tumor cells persist in the bone marrow of breast cancer patients through sustained activation of the unfolded protein response. Cancer Res. 2015;75:5367–77.
32. Carnesecchi J, Forcet C, Zhang L, Tribollet V, Barenton B, Boudra R, et al. ERRα induces H3K9 demethylation by LSD1 to promote cell invasion. Proc Natl Acad Sci USA. 2017;114:3909–14.
33. Deblois G, Smith H, Tam I, Gravel S, Caron M, Savage P, et al. ERRα mediates metabolic adaptations driving lapatinib resistance in breast cancer. Nat Commun. 2016;12:12156.
34. Stark C, Breitkreutz B, Reguly T, Boucher L, Breitkreutz A, Tyers M. BioGRID: a general repository for interaction datasets. Nucleic Acids Res. 2006;34:D535–9.
35. Zhang X, Wang Q, Gerald W, Hudis C, Norton L, Smid M, et al. Latent bone metastasis in breast cancer tied to Src-dependent survival signals. Cancer Cell. 2009;16:67–78.
36. Bieche I, Parfait B, Le Doussal V, Olivi M, Rio M, Lidereau R, et al. Identification of CGA as a novel estrogen receptor-responsive gene in breast cancer: an outstanding candidate marker to predict the response to endocrine therapy. Cancer Res. 2001;61:1652–8.
37. Sigl V, Owusu-Boaitey K, Joshi P, Kavirayani A, Wirnsberger G, Novatchkova M, et al. RANKL/RANK control Brca1 mutation-driven mammary tumors. Cell Res. 2016;26:761–74.
38. Castet A, Herledan A, Bonnet S, Jalaguier S, Vanacker JM, Cavailles V. Receptor-interacting protein 140 differentially regulates estrogen receptor-related receptor transactivation depending on target genes. Mol Endocrinol. 2006;20:1035–47.
39. Sumi D, Ignarro L. Sp1 transcription factor expression is regulated by estrogen-related receptor alpha1. Biochem Biophys Res Commun. 2005;328:165–72.

40. Zhang L, Teng Y, Zhang Y, Liu J, Xu L, Qu J, et al. Receptor activator for nuclear factor κ B expression predicts poor prognosis in breast cancer patients with bone metastasis but not in patients with visceral metastasis. J Clin Pathol. 2012;65:36–40.
41. Campbell J, Karolak M, Ma Y, Perrien D, Masood-Campbell S, Penner N et al. Stimulation of host bone marrow stromal cells by sympathetic nerves promotes breast cancer bone metastasis in mice. PLoS Biol [Internet]. 2012. https://doi.org/10.1371/journal.pbio.1001363
42. Blake M, Tometsko M, Miller R, Jones J, Dougall W. RANK expression on breast cancer cells promotes skeletal metastasis. Clin Exp Metastas. 2014;31:233–45.
43. Zeng R, Faccio R, Novack D. Alternative NF-κB regulates RANKL-induced osteoclast differentiation and mitochondrial biogenesis via independent mechanisms. J Bone Miner Res. 2015;30:2287–99.
44. Dirckx N, Tower R, Mercken E, Vangoitsenhoven R, Moreau-Triby C, Breugelmans T, et al. Vhl deletion in osteoblasts boosts cellular glycolysis and improves global glucose metabolism. J Clin Invest. 2018;128:1087–105.
45. Takeno A, Kanazawa I, Notsu M, Tanaka K, Sugimoto T. Glucose uptake inhibition decreases expressions of receptor activator of nuclear factor-kappa B ligand (RANKL) and osteocalcin in osteocytic MLO-Y4-A2 cells. Am J Physiol Endocrinol Metab. 2018;314:E115–23.
46. Barretina J, Caponigro G, Stransky N, Venkatesan K, Margolin A, Kim S, et al. The Cancer Cell Line Encyclopedia enables predictive modelling of anticancer drug sensitivity. Nature. 2012;483:603–7.
47. Salatino S, Kupr B, Baresic M, van Nimwegen E, Handschin C. The genomic context and corecruitment of SP1 affect ERRα coactivation by PGC-1α in muscle cells. Mol Endocrinol. 2016;30:809–25.
48. Nolan E, Vaillant F, Branstetter D, Pal B, Giner G, Whitehead L, et al. RANK ligand as a potential target for breast cancer prevention in BRCA1-mutation carriers. Nat Med. 2016;22:933–9.
49. Ishibashi H, Suzuki T, Suzuki S, Moriya T, Kaneko C, Takizawa T, et al. Sex steroid hormone receptors in human thymoma. J Clin Endocrinol Metab. 2003;88:2309–17.
50. Rakha E, El-Sayed M, Lee A, Elston C, Grainge M, Hodi Z, et al. Prognostic significance of nottingham histologic grade in invasive breast carcinoma. J Clin Oncol. 2008;26:3153–8.
51. Curtis C, Shah S, Chin S, Turashvili G, Rueda O, Dunning M, et al. The genomic and transcriptomic architecture of 2,000 breast tumours reveals novel subgroups. Nature. 2012;486:346–52.
52. Bos P, Zhang X, Nadal C, Shu W, Gomis R, Nguyen D, et al. Genes that mediate breast cancer metastasis to the brain. Nature. 2009;459:1005–9.
53. Wang Y, Klijn J, Zhang Y, Sieuwerts A, Look M, Yang F, et al. Gene-expression profiles to predict distant metastasis of lymph-node-negative primary breast cancer. Lancet. 2005;365:671–9.
54. Minn A, Gupta G, Siegel P, Bos P, Shu W, Giri D, et al. Genes that mediate breast cancer metastasis to lung. Nature. 2005;436:518–24.
55. Pantel K, Dickmanns A, Zippelius A, Klein C, Shi J, Hoechtlen-Vollmar W, et al. Establishment of micrometastatic carcinoma cell lines: a novel source of tumor cell vaccines. J Natl Cancer Inst. 1995;87:1162–8.
56. Bonnelye E, Saltel F, Chabadel A, Zirngibl RA, Aubin JE, Jurdic P. Involvement of the orphan nuclear estrogen receptor-related receptor alpha in osteoclast adhesion and transmigration. J Mol Endocrinol. 2010;45:365–77.
57. Chaveroux CEL, Dufour CR, Shatnawi A, Khoutorsky A, Bourque G, Sonenberg N, et al. Molecular and genetic cross-talks between mTOR and ERRα are key determinants of rapamycin-induced nonalcoholic fatty liver. Cell Metab. 2013;17:586–98.
58. David M, Ribeiro J, Descotes F, Serre CM, Barbier M, Murone M, et al. Targeting lysophosphatidic acid receptor type 1 with Debio 0719 inhibits spontaneous metastasis dissemination of breast cancer cells independently of cell proliferation and angiogenesis. Int J Oncol. 2012;40:1133–41.
59. Shannon P, Markiel A, Ozier O, Baliga N, Wang J, Ramage D, et al. Cytoscape: a software environment for integrated models of biomolecular interaction networks. Genome Res. 2003;13:2498–504.
60. Yevshin I, Sharipov L, Valeev T, Kel A, Kolpakov F. GTRD: a database of transcription factor binding sites identified by ChIP-seq experiments. Nucleic Acids Res. 2017;45:D61–7.
61. Delliaux C, Tian T, Bouchet M, Fradet A, Vanpouille N, Flourens A, et al. TMPRSS2:ERG gene fusion expression regulates bone markers and enhances the osteoblastic phenotype of prostate cancer bone metastases. Cancer Lett. 2018;438:32–43.